# Do Linear-Chain Perfluoroalkanes Bind an Electron?

**Ankan Paul, Chaitanya S. Wannere, and Henry F. Schaefer III***

*Center for Computational Quantum Chemistry, University of Georgia, Athens, Georgia 30602*

*Received: November 12, 2003; In Final Form: June 23, 2004*

The adiabatic electron affinities (AEAs), vertical electron affinities (VEAs), and vertical detachment energies (VDEs) of linear-chain perfluoroalkanes (PFAs), *n*-$C_nF_{2n+2}$ ($n = 2-8$) are predicted using carefully calibrated computational methods (*Chem. Rev.* **2002**, *102*, 231). Density functional theoretical methods and hybrid Hartree−Fock/density functional methods have been used with double-ζ-quality basis sets with polarization and diffuse functions, DZP++. Vibrational frequency analyses were performed to compute the zero-point energy corrections and determine the nature of the stationary points. The estimated adiabatic electron affinities of linear-chain PFAs ($C_nF_{2n+2}$), from $n = 3$ to $n = 8$, turn out to be appreciable, ranging from 0.26 to 0.58 eV (B3LYP/DZP++ method). The corresponding zero-point-corrected values are a bit larger, ranging from 0.39 to 0.71 eV. $C_2F_6$ is the only *n*-PFA exhibiting a negative adiabatic electron affinity. The trends in AEAs of the *n*-PFA show that the AEA increases with increasing chain length until $n = 7$ and then slightly decreases at $n = 8$. The VEAs of all the linear chain PFAs are negative. VEAs increase with increasing length of the linear-chain PFAs. The VDEs indicate that all the straight-chain PFA anions considered are bound with respect to electron loss. It was also observed that PFA molecules show enhanced AEAs when they are branched. The presence of tertiary C−F bonds in PFAs results in high AEAs compared to those of their straight-chain counterparts.

## Introduction

Perfluoroalkanes (PFAs) are used in numerous industrial applications.[1,2] Due to their chemical inertness, solvent resistance, extreme hydrophobicity, thermal stability, high lubricity, and low dielectric constant, PFAs are excellent candidates for inert solvents, lubricants, sealants, surfactants, oxygen carriers, and anesthetics.[3−9] Cyclic PFAs are replacing the previous choice, $SF_6$, as tracers in atmospheric dispersion studies.[10] The unusual solubility characteristics of PFAs have led to the emergence of a new field in catalytic chemistry known as fluorous biphase chemistry.[11] Given the strength of carbon−fluorine bonds in saturated systems and the lack of functionality, PFAs have generally been perceived to be chemically inert. PFAs have earned the dubious distinction of being "immortal molecules".[12] The low reactivity of PFAs is responsible for their long lifetime in the atmosphere, earning them membership in the notorious club of potential greenhouse gases.[13] Chemical innovations involving PFAs have broken the myth of "chemical inertness" of this class of molecules. In their seminal work on PFAs, about four decades ago, Tatlow and co-workers reported that defluorination of perfluoroalkanes can be achieved by activation of the C−F bonds.[14] Macnicol and Robertson showed that reactivity in perfluoroalkanes can be induced using arenethiolate nucleophiles under mild conditions.[15] PFAs do, in fact, have an interesting and developing chemistry originating from carbon−fluorine bond activation.[15−21] All the well-established reactions exploit the enhanced activity of the tertiary C−F bonds, which has been termed as the "Achilles heel" of PFAs, to initiate reductive defluorination.

The chemistry of perfluoroalkanes is dominated by the transfer of electrons. The different pathways that have been exploited to initiate chemistry in PFAs are electron attachment in the gas phase (negative ion mass spectrometry)[22−34] and electron transfer from metal surfaces (e.g., iron or other transition-metal complexes) or from electron-rich organic donors (e.g., thiolates)[15] to the σ* orbital of a C−F bond in the substrate. Such processes follow a radical anion mechanism, where loss of fluoride initiates a cascade of reactions leading to unsaturated products. For example, defluorination of perfluorodecalin is generally considered to occur by the transfer of electrons to the σ* orbital of the most electron deficient tertiary carbon−fluorine bond to give a radical anion. Loss of fluoride leads to a tertiary free radical which picks up another electron and forms a carbanion. This is followed by fluoride loss forming a double bond at the fused part of the two six-membered rings. Repeated electron transfer and fluoride elimination eventually lead to formation of octafluoronaphthalene.[35,36]

The preference for radical anion mechanisms in the defluorination reactions of PFAs suggests the presence of appreciable electron affinities in this class of molecules. The possibility of PFAs possessing appreciable electron affinities has made them important candidates for electron attachment and scattering studies.[22−34,37−39] Christophorou and co-workers have carried out extensive high-pressure electron attachment studies on linear-chain PFAs.[23−32] They have shown that low-energy electrons attach to *n*-PFAs dissociatively and/or nondissociatively depending on the chain length.[23,24,28] Parent negative ion formation was observed only for *n*-$C_nF_{2n+2}$, for $n = 3-6$.[24] Electron attachment to $CF_4$ and $C_2F_6$ was found to be dissociative in nature.[23,24] Moreover, it was noted that for branched *i*-$C_4F_{10}$ (perfluoroisobutane) the parent anion formation was much more abundant compared to that for *n*-$C_4F_{10}$.[23] Although comprehensive studies have been carried out on electron attachment rate coefficients of *n*-PFAs, there is a scarcity of scientific literature on the electron affinities of these molecules, on both the experimental and theoretical fronts. On the theoretical side, Leibman used molecular orbital considerations to

10.1021/jp0312417 CCC: $27.50 
Published on Web 10/01/2004

explain the higher electron affinities of cyclic perfluoroalkanes compared to their linear-chain counterparts.[40] King et al. have predicted, on the basis of hybrid HF/DFT methods, that $C_2F_6$ has a negative adiabatic electron affinity.[41] Moreover, their computations of vertical detachment energies for $C_2F_6$ reveal that this anionic species is unbound with respect to electron loss. Falcetta, Choi, and Jordan have carried out studies on negative ion states of $C_2F_6$ using ab initio techniques, and they have computed vertical electron affinities (VEAs) for $C_2F_6$.[42] Estimates of the VEAs of linear-chain PFAs and PFAs have been reported by Ishii et al. using the electron transmission (ETS) technique.[33] The plethora of experimental evidence that stable radical anion species can be formed from the larger perfluoroalkanes inspired us to initiate a theoretical investigation on straight-chain perfluoroalkanes. Currently there is no theoretical insight about the adiabatic electron affinity trends in *n*-PFAs and the structural features of the corresponding radical anion species. We have used a set of reliable density functional methods (pure and hybrid) to compute vertical and adiabatic electron affinities and vertical detachment energies for straight-chain $C_nF_{2n+2}$ ($n = 2-8$). Moreover, we have investigated the significant changes in electron affinity which occur on branching in two of these molecules, namely, $C_4F_{10}$ and $C_5F_{12}$.

## Methods

Energies, optimized structures, harmonic vibrational frequencies, and spin densities were obtained using three generalized gradient optimized (GGA) exchange correlation functionals, B3LYP, BLYP, and BP86. These are combinations of Becke's exchange correlation functionals, the three-parameter HF/DFT hybrid functional (B3)[43] or the pure exchange functional (B),[44] with the correlation functional of Lee, Young, and Parr (LYP)[45] or that of Perdew (P86).[46,47] All computations were performed using double-$\zeta$-quality basis sets with polarization and diffuse functions, DZP++. The DZP++ basis sets were constructed by augmenting the 1970 Huzinage−Dunning[48,49] sets of contracted double-$\zeta$ basis functions with one set of five d-type polarization functions for each C and F. In addition to this, even-tempered s- and p-type basis functions were added to each C and F. The even-tempered functions were designed following Lee and Schaefer's prescription:[50]

$$\alpha_{\text{diffuse}} = \frac{1}{2}\left(\frac{\alpha_1}{\alpha_2} + \frac{\alpha_2}{\alpha_3}\right)\alpha_1$$

where $\alpha_1$, $\alpha_2$, and $\alpha_3$ are the three smallest Gaussian orbital exponents of s- and p-type primitive functions for a given atom ($\alpha_1 < \alpha_2 < \alpha_3$). The final DZP++ set contains 19 functions per C and F atom (10s6p1d/5s3p1d). This basis set with the earlier mentioned DFT and hybrid HF/DFT methods has been used in systematic calibrative EA studies on a wide range of molecules.[51] The combination of the BLYP and B3LYP functionals with the DZP++ basis sets has been shown to predict electron affinities with average errors of less than 0.15 eV. In the present investigation restricted and unrestricted DFT methods were used for the neutral species and the anionic species, respectively. All structures were optimized employing analytic gradients with tight convergence criteria. Harmonic vibrational frequencies were computed without the application of any scaling factor. Numerical integration was performed using the Gaussian 94 default grid of 75 radial shells with 302 angular points per shell.[52] Adiabatic electronic affinities (AEAs) were computed as the difference between the appropriate neutral and anion species at their respective optimized geometries:

$$\text{AEA} = \text{energy(optimized neutral)} - \text{energy(optimized anion)}$$

The VEAs were computed as the energy difference between the neutral and the anion, at the neutral's optimized geometry:

$$\text{VEA} = \text{energy(optimized neutral)} - \text{energy(anion at the optimized neutral geometry)}$$

The vertical detachment energies (VDEs) were computed as the difference between the anion and the neutral, at the anion's optimized geometry:

$$\text{VDE} = \text{energy(neutral at the anion optimized geometry)} - \text{energy(optimized anion)}$$

For all anionic species, plots of total spin density were computed. This quantity is given, within the DFT approximations used here, by the difference in density of $\alpha$- and $\beta$-assigned electrons:

$$\rho^s(\mathbf{r}) = \rho^\alpha(\mathbf{r}) - \rho^\beta(\mathbf{r})$$

The total spin density allows us to examine the extent of delocalization of the unpaired electron within the molecular framework.

## Results and Discussion

The AEAs, VEAs, and VDEs are tabulated in Tables 1−3, respectively, while the optimized geometries of $C_2F_6$, $C_3F_4$, $C_4F_{10}$, and *i*-$C_4F_{10}$ and their corresponding anions are shown in Figures 1−4, respectively. A discussion of the EAs will ensue after the analysis of the optimized geometrical structures of the neutral and the anions. The optimized molecular geometries of all the other PFA molecules and their molecular anions studied are provided in the Supporting Information.

**A. Neutral Linear-Chain PFAs.** Jorgensen and co-workers have analyzed different conformations of $C_4F_{10}$, $C_5F_{12}$, and $C_6F_{14}$.[53] Perusal of the recent literature on perfluroalkanes reveals that a good amount of computational work has been done on the development of force fields and on conformational analysis for the linear-chain PFA molecules.[53−63] Following the literature on PFAs, we have arrived at our conformational choices for these molecules. It is known[53] that linear-chain PFAs prefer *all-trans* (staggered) conformations as the global minima. However, possible deviations from the ideal *all-trans* conformation may be expected due to destabilizing steric 1,5 diaxial interactions.[53] For the odd-numbered linear-chain PFAs ($C_nF_{2n+2}$, where *n* is odd) we have imposed $C_{2v}$ symmetry, while for the even-numbered (except for $n = 2$) linear-chain PFAs our preferred choice was $C_{2h}$ symmetry. Geometry optimizations of the linear-chain PFAs using all three density functionals and subsequent harmonic vibrational frequency analysis at the respective stationary points showed that all the linear-chain PFAs except $C_3F_8$ prefer a lower symmetry. Imposition of $C_{2v}$ symmetry for $C_5F_{12}$ and $C_7F_{16}$ and $C_{2h}$ symmetry for $C_4F_{10}$, $C_6F_{14}$, and $C_8F_{18}$ leads to small imaginary vibrational frequencies, which disappear when molecular geometries are allowed to distort to $C_2$ symmetry. Understandably, due to large conformational flexibility in these linear-chain PFAs, the corresponding potential energy surfaces are expected to be flat. In $C_3F_8$, where the number of 1,5 diaxial interactions is a minimum compared to that of other long-chain *n*-PFAs, a global minimum of $C_{2v}$ symmetry with the *all-trans* conformation is preferred. $C_3F_8$ prefers the *all-trans* (staggered) conformation

**TABLE 1: Adiabatic Electron Affinities of Linear-Chain $C_nF_{2n+2}$ (eV) ($n = 3-8$)[a]**

| molecule | B3LYP | BLYP | BP86 |
|---|---|---|---|
| $C_2F_6$ | −0.52 | −0.33 | −0.43 |
| | (−0.37) | (−0.19) | (−0.29) |
| $C_3F_8$ | 0.26 | 0.43 | 0.35 |
| | (0.39) | (0.56) | (0.48) |
| $C_4F_{10}$ | 0.40 | 0.57 | 0.50 |
| | (0.53) | (0.70) | (0.63) |
| $C_5F_{12}$ | 0.50 | 0.68 | 0.60 |
| | (0.65) | (0.83) | (0.74) |
| $C_6F_{14}$ | 0.56 | 0.73 | 0.67 |
| | (0.69) | (0.87) | (0.81) |
| $C_7F_{16}$ | 0.58 | 0.75 | 0.69 |
| | (0.71) | (0.89) | (0.83) |
| $C_8F_{18}$ | 0.52 | 0.71 | 0.64 |
| | (0.66) | (0.85) | (0.78) |

[a] Zero-point-corrected EAs are shown in parentheses.

**TABLE 2: Vertical Electron Affinities of Linear-Chain $C_nF_{2n+2}$ (eV) ($n = 2-8$)**

| molecule | B3LYP | BLYP | BP86 | expt 1[a] | expt 2[b] |
|---|---|---|---|---|---|
| $C_2F_6$ | −1.17 | −1.16 | −1.05 | | −4.6 |
| $C_3F_8$ | −1.03 | −0.96 | −0.96 | −2.55 | −3.34 |
| $C_4F_{10}$ | −0.92 | −0.77 | −0.78 | −1.95 | −2.37 |
| $C_5F_{12}$ | −0.85 | −0.60 | −0.61 | −1.55 | −1.64 |
| $C_6F_{14}$ | −0.63 | −0.36 | −0.36 | −1.20 | −1.20 |
| $C_7F_{16}$ | −0.53 | −0.19 | −0.20 | | |
| $C_8F_{18}$ | −0.36 | −0.07 | −0.06 | | |

[a] Hunter, S. R.; Christophorou, L. G. *J. Chem. Phys.* **1984**, *80*, 6150. [b] Ishii, I.; McLaren, R.; Hitchcock, A. P.; Jordan, K. D.; Choi, Y.; Robin, M. B. *Can. J. Chem.* **1988**, *66*, 2104.

**TABLE 3: Vertical Detachment Energies of Linear-Chain $C_nF_{2n+2}$ (eV) ($n = 2-8$)**

| molecule | B3LYP | BLYP | BP86 |
|---|---|---|---|
| $C_2F_6$ | 3.08 | 2.81 | 2.68 |
| $C_3F_8$ | 3.41 | 3.31 | 3.16 |
| $C_4F_{10}$ | 3.43 | 3.24 | 3.16 |
| $C_5F_{12}$ | 3.50 | 3.31 | 3.23 |
| $C_6F_{14}$ | 3.51 | 3.31 | 3.21 |
| $C_7F_{16}$ | 3.55 | 3.33 | 3.23 |
| $C_8F_{18}$ | 3.65 | 3.42 | 3.32 |

since the bond dipole−dipole repulsions are minimized and dominate over 1,5 diaxial interactions, making the staggered conformation of $C_3F_8$ a global minimum. The gas-phase experimental structure of *n*-$C_3F_8$ has been reported as the staggered conformer.[64] With the growth in carbon chain length, the number of 1,5 diaxial interactions increases, causing deviations from the staggered conformations. Dixon has shown in his work on the torsional potential about the central C−C bond in perfluoro-*n*-butane that the global conformational minimum is a twist-anti form. The latter structure shows a twist in the carbon backbone by an angle of 15° about the central C−C bond (away from the 180° for the *all-trans* structure) at the SCF level with a 6-31G* basis set.[57,58] The optimized geometry at B3LYP/DZP++ exhibits a similar twist of 13° in the carbon backbone about the central C−C bond. All the long-chain *n*-PFAs from $n = 4$ to $n = 8$ show similar deviations. The twist angle in the C−C backbone of *n*-$C_4F_{10}$ predicted by the current work is in satisfactory agreement with the previously reported MP2- and B3LYP-optimized geometries.[53,54,58,59] Our optimized structures for the longer neutral *n*-PFAs with $C_2$ symmetry show that the *n*-PFA backbone is helical in nature, in concordance with previous reports in the literature.[53,54] Information about the dihedral angles along the C−C backbones of the *n*-PFAs is provided in the Supporting Information.

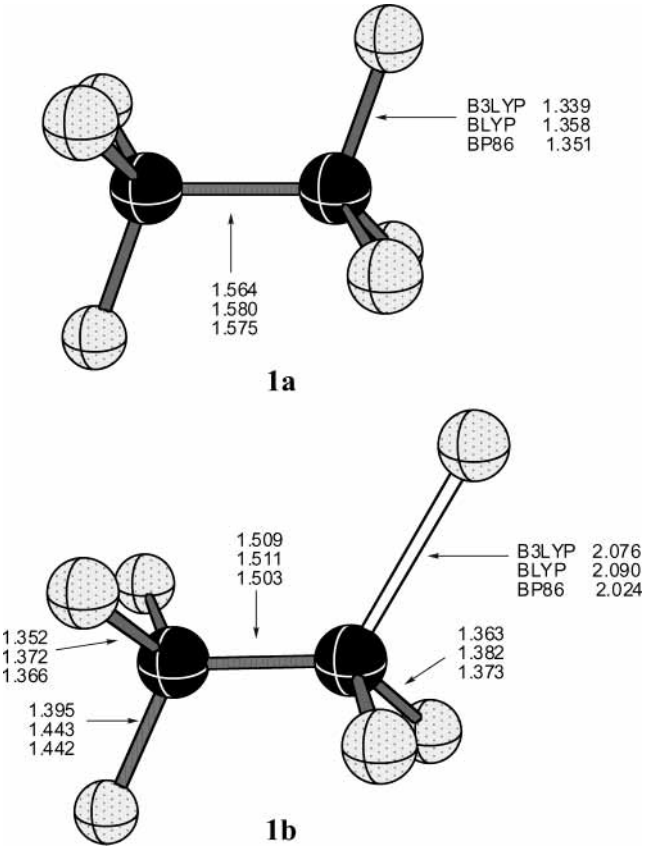


**Figure 1.** Optimized molecular geometries of (a, top) neutral *n*-$C_2F_6$ ($D_{3d}$ symmetry) and (b, bottom) anionic *n*-$C_2F_6^-$ ($C_s$ symmetry). All bond lengths reported are in angstroms.

Analysis of the bond lengths shows that the B3LYP method predicts the shortest bond lengths for both C−C and C−F bonds among all three functionals, whereas BLYP predicts the longest bonds.

**B. Anions of Linear-Chain PFAs.** The optimized bond lengths and the corresponding molecular geometries of *n*-$C_nF_{2n+2}^-$ ($n = 2$, 3, and 4) are indicated in Figures 1b−3b, respectively. The study of the optimized structures of the molecular anions reveals that drastic changes occur within the molecular framework on electron attachment. The linear-chain PFA anions show a consistent change in geometry compared to their corresponding neutral species. The most conspicuous change occurs for one of the C−F bonds, namely, that located on the central carbon for the odd-numbered *n*-PFA anion and on one of the central carbons in even-numbered *n*-PFA anions. Molecular geometry optimization using three different functionals (with subsequent vibrational frequency analysis) imposing $C_{2v}$ symmetry on $C_nF_{2n+2}^-$, where *n* is odd, leads to a single large imaginary frequency which shows distortion toward the asymmetric stretch of the C−F bonds on the central $-CF_2$ unit. While $C_3F_8^-$ and $C_7F_{14}^-$ prefer $C_s$ symmetry, $C_5F_{12}^-$ prefers $C_1$ geometry. Imposing $C_s$ symmetry on $C_5F_{12}^-$ followed by geometry optimization and harmonic frequency analysis shows the presence of a very small imaginary frequency at all levels of theory (e.g., 11i $cm^{-1}$ at B3LYP/DZP++), which corresponds to torsional twisting of the $-CF_2$ units in the molecular framework. In all the odd-numbered PFA anions significant C−F bond length elongation occurs on one of the two C−F bonds located in the center of the chain. For example, with B3LYP/DZP++ the C−F bond length in question in $C_3F_8^-$ is exceptionally long, 2.046 Å (Figure 2b), whereas at the same level of theory the C−F bond length in the neutral molecule has a typical value,

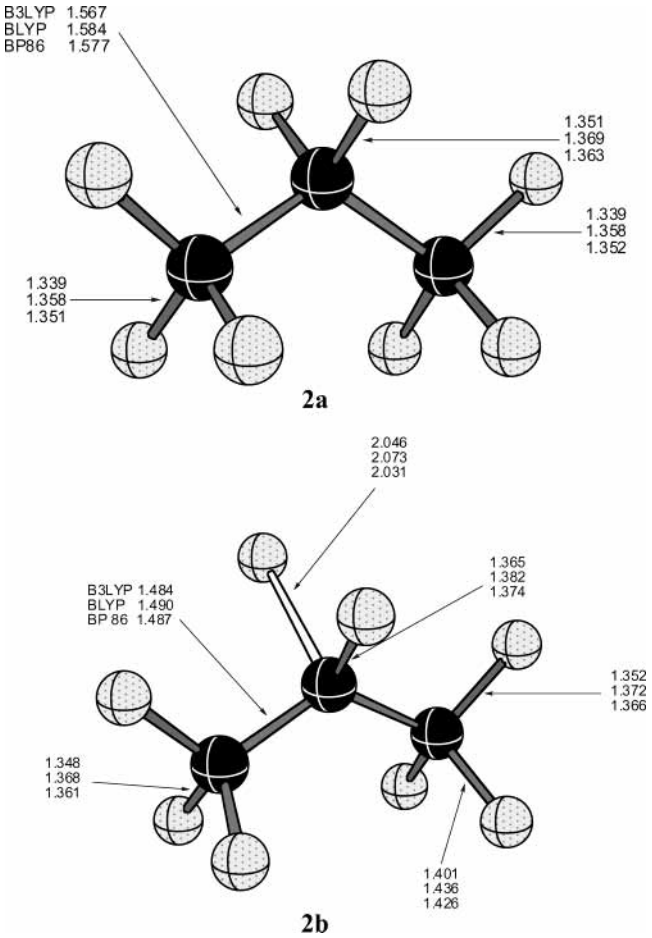


**Figure 2.** Optimized molecular geometries of (a, top) neutral *n*-$C_3F_8$ ($C_{2v}$ symmetry) and (b, bottom) anionic *n*-$C_3F_8^-$ ($C_s$ symmetry). All bond lengths reported are in angstroms.

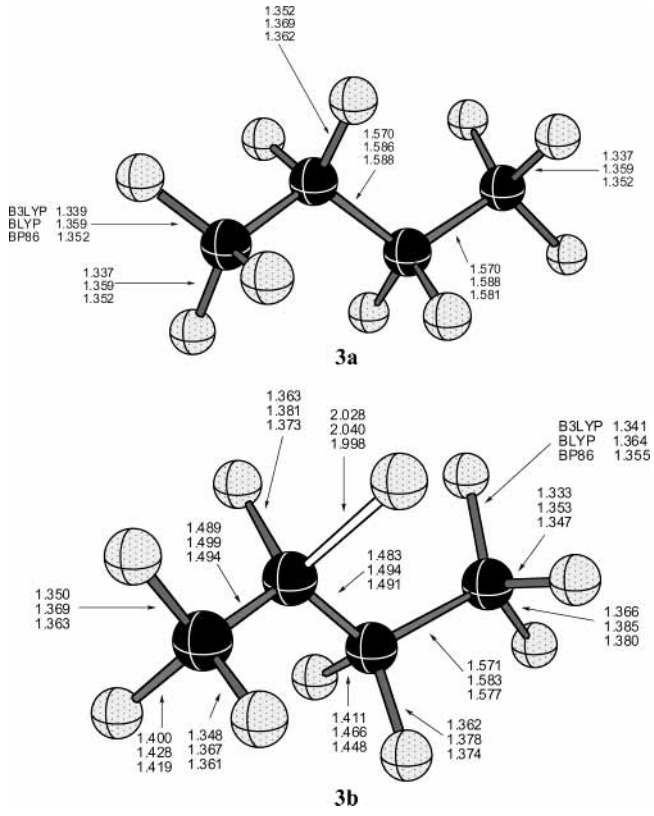


**Figure 3.** Optimized molecular geometries of (a, top) neutral *n*-$C_4F_{10}$ ($C_2$ symmetry) and (b, bottom) anionic *n*-$C_4F_{10}^-$ ($C_1$ symmetry). All bond lengths reported are in angstroms.

1.351 Å. In $C_5F_{12}^-$, the longest C−F bond has a length of 2.012 Å and the longest C−F bond in $C_7F_{16}^-$ measures up to 2.009 Å at the B3LYP/DZP++ level of theory. Moreover, there is C−C bond shortening in the anionic species compared to their neutral analogues for the C−C bonds, which are associated with the central carbon in the chain. The C−C bond distances associated with the central carbon in $C_3F_8^-$ are about 1.484 Å at the B3LYP/DZP++ level, whereas in the neutral $C_3F_8$ the same C−C bond has slightly longer distance, 1.567 Å. In addition, C−F bonds that are *trans* to the longest C−F bonds also are slightly elongated compared to the quasi-*syn* ones. Similar bond length patterns are also observed in the other odd-numbered *n*-PFA anions.

The structural features of even-numbered *n*-PFA anions are similar in nature to those of the odd-numbered chains. The optimized structures of all the even-numbered *n*-PFA anions exhibit an exceptionally long C−F bond, which is located on one of the central carbons in the chain. $C_2F_6^-$ prefers a $C_s$ structure (Figure 1b) and the other even-numbered *n*-PFA anions prefer $C_1$ structures as minima. Analysis of the optimized geometries of $C_4F_{10}^-$ (Figure 3a) at all three levels of theory reveals the presence of an exceptionally long C−F bond (2.028 Å at B3LYP/DZP++) on the second carbon from the end of the chain. In the vicinity of the exceptionally long C−F bond in $C_4F_{10}^-$, we observe C−C bond shortening and slight elongation of the C−F bond *trans* to the longest C−F bond, similar to those observed for the odd-numbered PFA anions. All the other even-numbered *n*-PFA anions show similar structural features. The longest C−F bond in $C_6F_{14}^-$ is associated with the third carbon from the end of the chain, and for $C_8F_{18}^-$ the fourth carbon from the end of the chain holds the longest C−F bond. In $C_6F_{14}^-$ the longest C−F bond has a length of 2.006 Å and the longest C−F bond in $C_8F_{18}^-$ is 2.030 Å long at the B3LYP/DZP++ level of theory. For $C_4F_{10}^-$ and $C_6F_{14}^-$ we were able to detect other low-lying minima possessing $C_{2h}$ symmetry. The $C_{2h}$ minimum for the $C_4F_{10}^-$ anion lies above the $C_1$ structure by 17 kcal/mol, whereas the $C_{2h}$ minimum for $C_6F_{14}^-$ is 13 kcal/mol higher in energy than the $C_1$ minimum (B3LYP/DZP++).

The structural changes that occur on attaching an electron to a PFA may be explained with the help of spin density plots. All the spin density plots for the molecular anions (Figure 5) were obtained at the B3LYP/DZP++ level of theory. For all the *n*-PFA anions the spin density is mainly associated with their corresponding longest C−F bonds. The elongation of the C−F bonds is due to the addition of an extra electron to an antibonding C−F $\sigma^*$ orbital. An increase in the electron density in the C−F $\sigma^*$ orbital leads to a lengthening of the respective C−F bond. The shortening of the C−C bonds which are associated with the carbon bearing the exceptionally long C−F bond, and also the observed lengthening of the C−F bonds *trans* to the longest C−F bond, can be explained on the basis of a negative hyperconjugation-like phenomenon. The half-filled C−F $\sigma^*$ orbital corresponding to the longest C−F bond in the anions mentioned above may have substantial overlap with the empty *trans* C−F $\sigma^*$ orbital. This in effect leads to a negative hyperconjugation-like phenomenon (see Figure 6). In Figure 6 we show how the overlap of a half-filled C−F $\sigma^*$ orbital with an empty C−F $\sigma^*$ orbital *trans* to it can lead to C−F bond lengthening and C−C bond shortening.

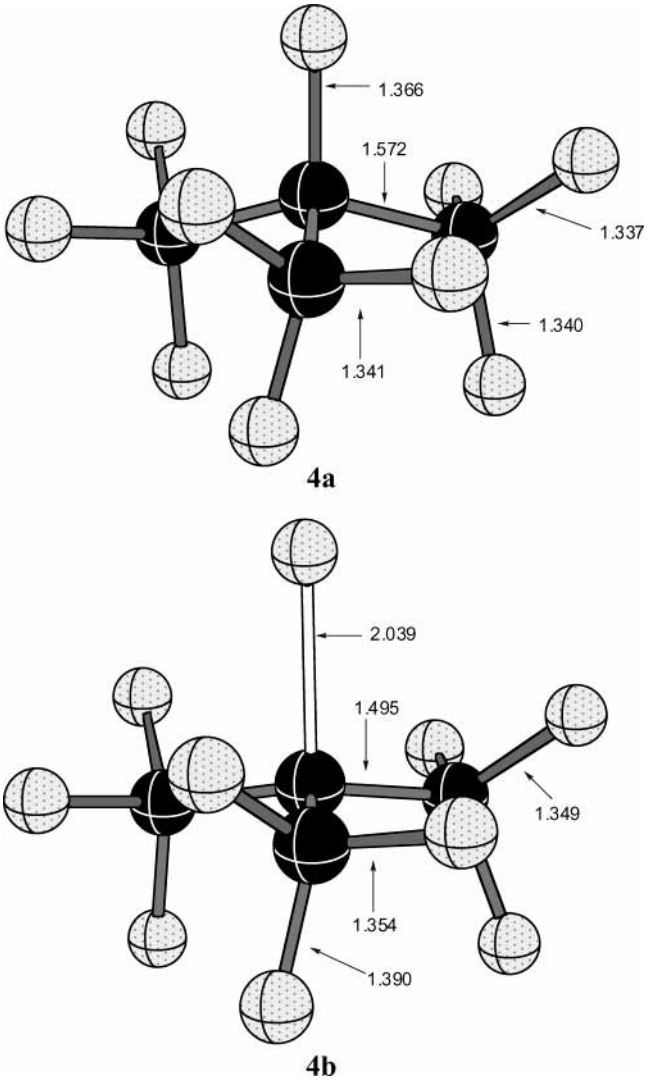


**Figure 4.** Optimized molecular geometries at the B3LYP/DZP++ level of theory: (a, top) neutral branched $C_4F_{10}$ ($C_3$ symmetry), (b, bottom) anionic branched $C_4F_{10}^-$ ($C_3$ symmetry). All bond lengths reported are in angstroms.

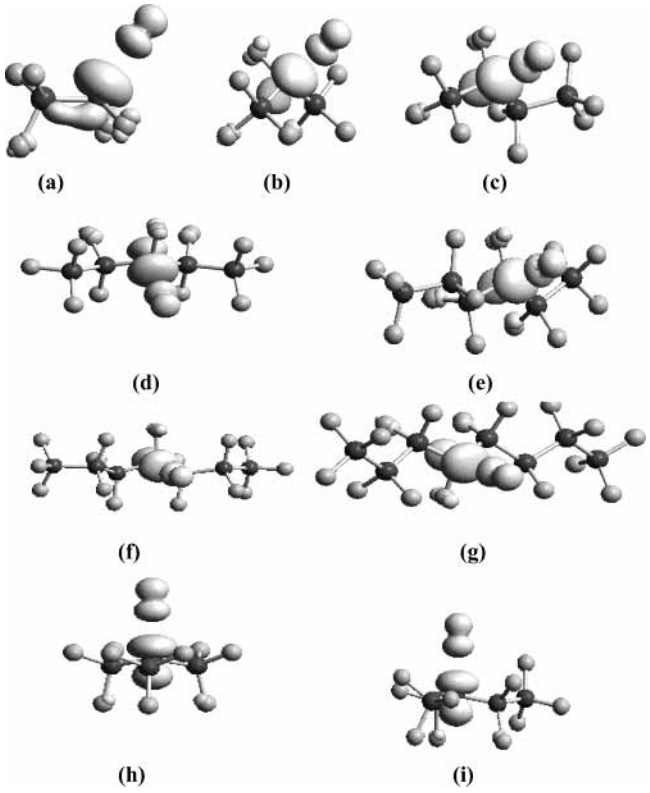


**Figure 5.** Spin density plots for molecular anions at B3LYP/DZP++: (a) *n*-$C_2F_6^-$ (b) *n*-$C_3F_8^-$, (c) *n*-$C_4F_{10}^-$, (d) *n*-$C_5F_{12}^-$, (e) *n*-$C_6F_{14}^-$, (f) *n*-$C_7F_{16}^-$, (g) *n*-$C_8F_{18}^-$, (h) branched $C_4F_{10}^-$, (i) branched $C_5F_{12}^-$.

**C. Electron Affinities of Linear-Chain PFAs.** Examination of the AEA data in Table 1 reveals that the BLYP method rather consistently predicts the highest EAs for all the species, while B3LYP estimates for the AEAs are the lowest. The zero-point-corrected AEAs are consistently higher than the corresponding uncorrected values. This of course reflects the smaller ZPVEs of the anions. The AEA predictions show a monotonic increase with increasing chain length for *n*-$C_nF_{2n+2}^-$, from $n = 2$ to $n = 7$. $C_8F_{18}$ and $C_7F_{16}$ have similar AEA values. All the linear-chain PFAs, with the exception of $C_2F_6$, have positive AEAs. The high-pressure electron attachment studies on straight-chain *n*-PFAs reveal that for $n > 2$ nondissociative electron attachment occurs.[23,24] $C_2F_6$ undergoes only dissociative electron attachment, whereas the other longer chain *n*-PFAs exhibit both dissociative and nondissociative electron attachment.[24] On the basis of electron attachment studies of $C_3F_8$, $C_4F_{10}$, $C_5F_{12}$, and $C_6F_{14}$, Christophorou and co-workers have suggested that these molecules possess positive electron affinities.[23,24,26,29,30] Our findings lend an explanation to their experimental observation. As noted earlier, the extra electron in the *n*-PFA anionic species occupies the C−F $\sigma^*$ orbital. The presence of the more negative inductive effect exerting $CF_2$ groups may lower the energy of the C−F $\sigma^*$ orbital, leading to an increase in AEA. The extra electron goes to the central carbon C−F bond for odd-carbon-containing PFA anions. For even-carbon PFA anions, the "last" electron goes to the C−F bond on one of the central carbons, as those specific carbons have the maximum number of $-CF_2$ groups in their vicinity. From $C_2F_6$ to $C_7F_{16}$ the AEA increases as the number of negative inductive effect exerting $-CF_2$ units increases. The incremental change in AEA along the series of *n*-PFA decreases as we move from $n = 2$ to $n = 7$. This can be rationalized by the understanding that the increase in the negative inductive effect on addition of $-CF_2$ units away from the electron-binding center weakens with increasing chain length. As one moves from $C_7F_{16}$ to $C_8F_{18}$ we observe that the increase in AEA ceases, plausibly pointing to the idea that further addition of $-CF_2$ groups far away from the electron-binding center has a negligible effect.

The VEAs show a similar trend. None of the straight-chain PFAs investigated have a positive VEA. Analysis of the predictions shows that the VEA increases with the chain length of the PFAs. The VEA results indicate that among the neutral straight-chain PFA molecules the LUMO is high lying. The LUMO energy is lowered with chain length growth due to the increase in the number of negative inductive effect exerting $CF_2$ groups.[33] The observed trend in VEA is in agreement with the previous experimental reports.[24,33] Though all three density functionals predict the right trend, they consistently overestimate the VEAs compared to the experimentally reported values.[24,33] The VEA data reveal that, if a linear-chain PFA has to bind an electron adiabatically, it has to lower the energy of its LUMO. We observe through molecular geometry optimization of the molecular anions that drastic changes within the molecular framework take place upon electron attachment. Bond elongation leads to a lowering of the energy of the corresponding

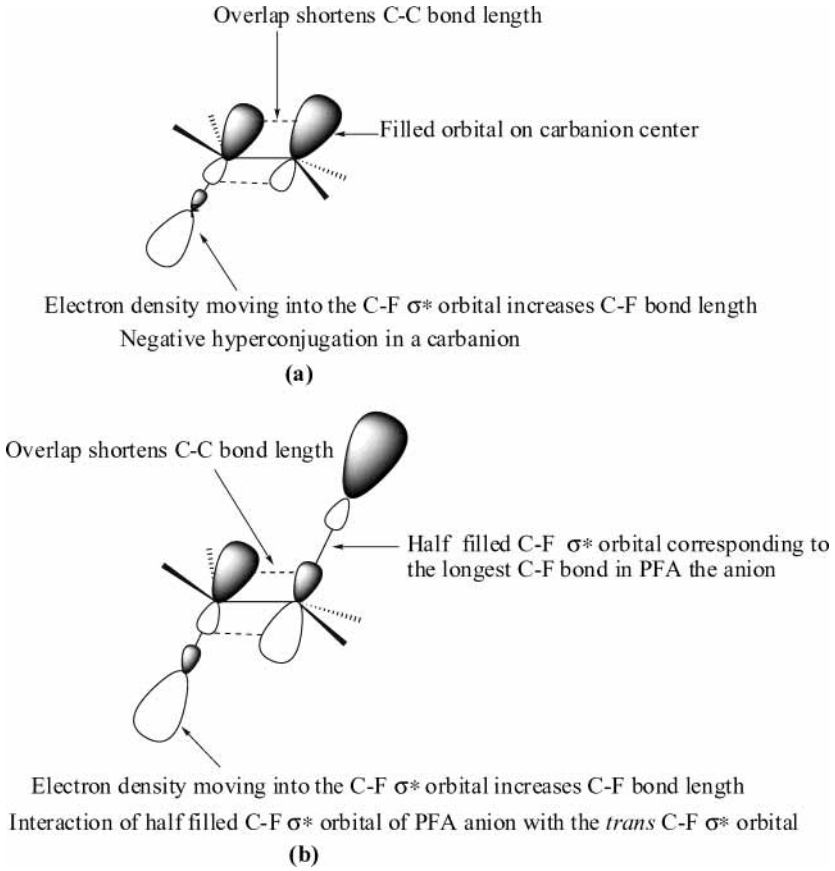


**Figure 6.** Comparison (for linear-chain PFA anions) between (a) negative hyperconjugation in carbanions and (b) the half-filled C−F $\sigma^*$ interaction with an empty *trans* C−F $\sigma^*$ orbital.

**TABLE 4: Comparison of the AEAs (eV) of Branched-Chain PFAs to Those of Their Straight-Chain Analogues**[a]

| method | branched $C_4F_{10}$ | *n*-$C_4F_{10}$ | branched $C_5F_{12}$ | *n*-$C_5F_{12}$ |
|---|---|---|---|---|
| B3LYP/DZP++ | 1.11 (1.23) | 0.40 (0.53) | 1.21 (1.33) | 0.50 (0.65) |

[a] Zero-point-corrected EAs are shown in parentheses.

antibonding $\sigma^*$ orbital, giving rise to a low-energy orbital that can efficiently bind an electron.

The VDEs indicate that all the molecular anionic species considered in this work are bound with respect to electron loss. Earlier it was demonstrated by King et. al. that $C_2F_6^-$ is unbound with respect to *electron loss*.[41] King et al. based their predictions on a $D_{3d}$ geometry for the $C_2F_6^-$ anion. In contrast to their results, we have found that a $C_s$ structure is the global minimum for the $C_2F_6^-$ anion. The $C_s$ minimum is 15 kcal/mol energetically lower than the $D_{3d}$ minimum at the B3LYP/DZP++ level of theory! When the optimized $C_s$ geometry of $C_2F_6^-$ is taken into consideration for the VDE computations, we find that it has a positive VDE, indicating $C_2F_6$ may form a bound anion. The high predicted VDEs for the longer chains show that all these molecular anions can exist.

**D. Electron Affinities of Branched-Chain $C_4F_{10}$ and $C_5F_{12}$.** The theoretical AEAs of branched $C_4F_{10}$ (perfluoroisobutane, *i*-$C_4F_{10}$) and $C_5F_{12}$ (perfluoroisopentane, *i*-$C_5F_{12}$) are listed in Table 4. Branched $C_4F_{10}$ has a much higher AEA than the linear-chain *n*-$C_4F_{10}$ (1.09 eV and 0.40 eV, respectively). This trend persists for the AEAs of the $C_5F_{12}$ isomers. The optimized anionic *i*-$C_4F_{10}^-$ shows a substantial elongation of the tertiary C−F bond (2.039 Å) (see Figure 4b) as compared to that for the neutral $C_3$ symmetry structure (1.366 Å) (see Figure 4a). The tertiary C−F bond is the longest bond in the molecular anion of branched $C_4F_{10}^-$. Tertiary C−F bond length elongation is also observed in *i*-$C_5F_{12}^-$. This prediction lends support to the generally accepted mechanism of defluorination of perfluorodecalin by reducing agents such as Na in organic media, where it is believed that a molecular anion is formed, followed by cleavage of the tertiary C−F bond.[35,36] Christophorou and coworkers reported the formation of a stable parent anion species on electron attachment to *i*-$C_4F_{10}$.[23] Our predicted geometry for *i*-$C_4F_{10}^-$ is a plausible molecular structure for the parent anion species formed on electron attachment to *i*-$C_4F_{10}$. The lengthening of the tertiary C−F bond in the molecular anion of *i*-$C_4F_{10}$ also indicates that a defluorination step will involve cleavage of the exceptionally long tertiary C−F bond in the subsequent step.[35,36] In branched $C_5F_{12}$ there is one C−F tertiary bond along with secondary and primary C−F bonds. In the optimized molecular geometry of the anion at B3LYP/DZP++ again we encounter an exceptionally long tertiary C−F bond. This indicates that the extra electron prefers to go to the tertiary C−F bond. The spin density plots (see Figure 5) for the branched anions reveal that the extra electron is accommodated in their tertiary C−F $\sigma^*$ orbitals. The enhanced AEA of PFA with tertiary C−F bonds may be explained on the basis of the tertiary C−F bonds having the maximum number of negative hyperconjugative effect exerting C−F bonds *trans* to it. Through the negative hyperconjugative effect the empty C−F $\sigma^*$ orbitals *trans* to the longest C−F bond help to delocalize the extra charge through $\sigma^*-\sigma^*$ interactions between the C−F bonds, as demonstrated earlier. The geometric changes in moving from the branched neutrals to the branched anions show the same structural effects as expected from negative hyperconjugation,

the shortening of the C−C bond associated with elongated C−F bond bearing carbon and the lengthening of the C−F bonds which are *trans* in orientation to the elongated C−F bonds.

## Concluding Remarks

Through this work we have shown that the straight-chain PFAs (with the exception of $C_2F_6$) have substantial adiabatic electron affinities. In addition, the VEA predictions reveal that none of the straight-chain PFAs possess a positive VEA. Moreover, the VEA increases with extension of the chain length of a PFA. Analysis of the VDE data shows that all the straight-chain molecular anions considered in this research are bound with respect to electron loss. The $C_2F_6^-$ anion, which was thought to possess a negative VDE,[41] has a more energetically favorable $C_s$ minimum which possesses a positive VDE. Spin density studies of the anions convincingly establish that the *n*-PFAs bind the extra electron in a C−F $\sigma^*$ antibonding orbital. It was also observed that branched PFAs possessing tertiary C−F bonds have much higher AEAs compared to their straight-chain analogues, indicating that branched-chain molecules can be better candidates for electron attachment studies.

**Acknowledgment.** A.P. thanks Dr. Alexey Timoshkin and Mr. Lubos Horny for their insightful comments and discussions. This research was supported by the National Science Foundation under Grant CHE-0136184.

**Supporting Information Available:** Optimized molecular geometries of $C_5F_{12}$, $C_6F_{14}$, $C_7F_{16}$, $C_8F_{18}$, and *i*-$C_2F_{12}$ and their corresponding anions (Figures S1−S5) and dihedral angles along the C−C backbone in the neutral *n*-PFA molecules (Table S1). This material is available free of charge via the Internet at http://pubs.acs.org.

## References and Notes

(1) Slinn, D. S. L.; Green, S. W. In *Preparation, Properties and Industrial Applications of Organofluorine Compounds*; Banks, R. E, Ed.; Ellis Horwood: Chichester, U.K., 1982; p 45.
(2) Green, S. W.; Slinn, D. S. L.; Simpson, R. N. F.; Woytek, A. J. In *Organofluorine Chemistry, Principles and Commercial Applications*; Banks, R. E., Smart, B. E., Tatlow, J. C., Eds.; Plenum: New York, 1994; p 89.
(3) Barthel-Rosa, L. P.; Gladysz, J. A. *Coord. Chem. Rev.* **1999**, *190*−*192*, 587.
(4) Kajdas, C. Industrial Lubricants. In *Chemistry and Technology of Lubricants*; Mortier, R. M., Orszulik, S. T., Eds.; VCH Publishers: New York, 1992.
(5) Eastoe, J.; Bayazit, Z.; Martel, S.; Steytler, D. C.; Heenan, R. K. *Langmuir* **1996**, *12*, 1423.
(6) Ogino. K.; Abe, M. *Mixed Surfactant Systems*; M. Dekker, Inc.: New York, 1993.
(7) Eger, E. I.; Jonescu, P.; Laster, M. J.; Gong, D.; Hudlicky, T.; Kending, J. J.; Harris, A.; Trudell, J. R.; Pohorille, A. *Anesth. Analg. (Baltimore)* **1999**, *88*, 867.
(8) Riess, J. G. *Chem. Rev.* **2001**, *101*, 2797.
(9) Spahn, D. R. *Adv. Drug. Delivery Rev.* **2000**, *40*, 143.
(10) Simmonds, P. G.; Greally, B. R.; Olivier, S.; Nickless, G.; Cook. K. M.; Dietz, R. N. *Atmos. Environ.* **2002**, *36*, 2147.
(11) Horvath, I. T. *Acc. Chem Res.* **1998**, *31*, 641.
(12) Ravishankara, A. R.; Solomon, S.; Turnispeed, A. A.; Warren, R. F. *Science* **1993**, *259*, 194.
(13) U.S. Greenhouse Gas Inventory Program, Office of Atmospheric Programs. Greenhouse Gases and Global Warming Potential Values. Excerpt from *Inventory of US Greenhouse Gas Emissions and Sinks: 1999*−*2000*; EPA-430-R-02-003; U.S. Environmental Protection Agency: Washington, DC, 2002.
(14) Coe, P. L.; Patrick, C. R. Tatlow, J. C. *Tetrahedron* **1960**, *9*, 240.
(15) Macnicol, D. D.; Robertson, C. D. *Nature* **1988**, *332*, 59.
(16) Richmond, T. G. *Angew. Chem., Int. Ed.* **2000**, *39*, 3241.
(17) Burdeniuc, J.; Jedlicka, B.; Crabtree, R. H. *Chem. Ber.* **1997**, *130*, 145.
(18) Kiplinger, G. L.; Richmond, T. G.; Ostreberg, C. E. *Chem. Rev.* **1994**, *94*, 373.
(19) Saunders, G. C. *Angew. Chem., Int. Ed. Engl.* **1996**, *35*, 2615.
(20) Richmond, T. G. *Top. Organomet. Chem.* **1999**, *3*, 243.
(21) Ogawa, A. *Organomet. News* **2001**, *1*, 17.
(22) Stoffels, E.; Stoffels, W. W.; Tachibana, K. *Rev. Sci. Instrum.* **1998**, *69*, 116.
(23) Spyrou, S. M.; Sauers, I.; Christophorou, L. G. *J. Chem. Phys.* **1983**, *78*, 7200.
(24) Hunter, S. R.; Christophorou, L. G. *J. Chem. Phys.* **1984**, *80*, 6150.
(25) Spyrou, S. M.; Christophorou, L. G. *J. Chem. Phys.* **1985**, *82*, 2620.
(26) Spyrou, S. M.; Christophorou, L. G. *J. Chem. Phys.* **1985**, *83*, 2829.
(27) Hunter, S. R.; Carter, J. G.; Christophorou, L. G. *J. Chem. Phys.* **1987**, *86*, 693.
(28) Hunter, S. R.; Carter, J. G.; Christophorou, L. G. *Phys. Rev. A* **1988**, *38*, 58.
(29) Datskos, P. G.; Christophorou, L. G. *J. Chem. Phys.* **1987**, *86*, 1982.
(30) Christophorou, L. G.; Olthoff, J. K. *J. Phys. Chem. Ref. Data* **1998**, *27*, 889.
(31) Christophorou, L. G.; Olthoff, J. K. *J. Phys. Chem. Ref. Data* **1998**, *27*, 1.
(32) Christophorou, L. G.; Olthoff, J. K. *J. Phys. Chem. Ref. Data* **1999**, *28*, 967.
(33) Ishii, I.; McLAren, R.; Hitchcock, A. P.; Jordan, K. D.; Choi, Y.; Robin, M. B. *Can. J. Chem.* **1988**, *66*, 2104.
(34) Weik, F.; Illenberger, E. *J. Chem. Phys.* **1995**, *103*, 1406.
(35) Marsella, J. A.; Gilicinski, A. G.; Coughlin, A. M.; Pez, G. P. *J. Org. Chem.* **1992**, *57*, 2856.
(36) Sung, K.; Lagow, R. J. *J. Chem. Soc., Perkin. Trans.* **1998**, *1*, 637.
(37) Nishimura, H.; Nishimura, F.; Nakamura, Y.; Okuda, K. *J. Phys. Soc. Jpn.* **2003**, *72*, 1080.
(38) Sanabia, J. E.; Cooper G. D.; Tossell, J. A.; Moore, J. H. *J. Chem. Phys.* **1998**, *108*, 389.
(39) Tanaka, H.; Tachibana, Y.; Kitajima, M.; Sueoka, O.; Takaki, H.; Hamada, A.; Kimura, M. *Phys. Rev. A* **1999**, *59*, 2006.
(40) Liebman, J. L. *J. Fluorine Chem.* **1973**, *3*, 27.
(41) King, R. A.; Pettigrew, N. D.; Schaefer, H. F. *J. Chem. Phys.* **1997**, *107*, 8536.
(42) Falcetta, M. F.; Choi, Y.; Jordan, K. D. *J. Phys. Chem. A* **2000**, *104*, 9605.
(43) Becke, A. D. *J. Chem. Phys.* **1993**, *98*, 5648.
(44) Becke, A. D. *Phys. Rev. A* **1988**, *38*, 3098.
(45) Lee, C.; Yang, W.; Parr, R. G. *Phys. Rev. B* **1988**, *37*, 785.
(46) Perdew, J. P. *Phys. Rev. B* **1986**, *33*, 8822.
(47) Perdew, J. P. *Phys. Rev. B* **1986**, *34*, 7406.
(48) Dunning, T. H. *J. Chem. Phys.* **1970**, *53*, 2823.
(49) Huzinaga, S. *J. Chem. Phys.* **1965**, *42*, 1293.
(50) Lee, T. J.; Schaefer, H. F. *J. Chem. Phys.* **1985**, *83*, 1784.
(51) Rienstra-Kiracofe, C. J.; Tschumper, G. S.; Schaefer, H. F. *Chem. Rev.* **2002**, *102*, 231.
(52) Frisch, M. J.; Trucks, G. W.; Schlegel, H. B.; Gill, P. M. W.; Johnson, B. G.; Robb, M. A.; Cheeseman, J. R.; Keith, T.; Petersson, G. A.; Montgomery, J. A.; Raghavachari, K.; Al-Laham, M. A.; Zakrzewski, V. G.; Ortiz, J. V.; Foresman, J. B.; Cioslowski, J.; Stefanov, B. B.; Nanayakkara, A.; Challacombe, M.; Peng, C. Y.; Ayala, P. Y.; Chen, W.; Wong, M. W.; Andres, J. L.; Replogle, E. S.; Gomperts, R.; Martin, R. L.; Fox, D. J.; Binkley, J. S.; Defrees, D. J.; Baker, J.; Stewart, J. P.; Head-Gordon, M.; Gonzalez, C.; Pople, J. A. *Gaussian 94*, revision E.2; Gaussian, Inc.: Pittsburgh, PA, 1995.
(53) Watkins, E. K.; Jorgensen, W. L. *J. Phys. Chem. A* **2001**, *105*, 4118.
(54) Borodin, O.; Smith, G. D.; Bedrov, D. *J. Phys. Chem. B* **2002**, *106*, 9912.
(55) Röthlisberger, U.; Laasonen, K.; Klein, M. L.; Sprik, M. *J. Chem. Phys.* **1996**, *104*, 3692.
(56) Sprik, M.; Röthlisberger, U.; Klein, M. L. *Mol. Phys.* **1999**, *97*, 355.
(57) Dixon, D. A.; Van Catledge, F. A. *Int. J. Supercomput. Appl.* **1988**, *2*, 52.
(58) Dixon, D. A. *J. Phys. Chem.* **1992**, *96*, 3698.
(59) Smith, G. D.; Jaffe, R. L.; Yoon, D. Y. *Macromolecules* **1994**, *27*, 3166.
(60) Albinsson, B.; Milch, J. *J. Phys. Chem.* **1996**, *100*, 3418.
(61) Albinsson, B.; Milch, J. *J. Am. Chem. Soc.* **1995**, *117*, 6378.
(62) Neumann, F.; Teramae, H.; Downing, J. W.; Milch, J. *J. Am. Chem. Soc.* **1998**, *120*, 573.
(63) Okada, O.; Oka, K.; Kuwajima, S.; Tanabe, K. *Mol. Simul.* **1999**, *21*, 325.
(64) Mack, H. G.; Dakkouri, M.; Oberhammer, H. *J. Phys. Chem.* **1991**, *95*, 3136.